THE JOURNAL OF BIOLOGICAL CHEMISTRY VOL. 285, NO. 8, pp. 5522–5531, February 19, 2010

Myosin Light Chain Kinase Is Necessary for Tonic Airway Smooth Muscle Contraction*

Received for publication, September 4, 2009, and in revised form, December 13, 2009 Published, JBC Papers in Press, December 14, 2009, DOI 10.1074/jbc.M109.062836

Wen-Cheng Zhang[‡], Ya-Jing Peng[‡], Gen-Sheng Zhang[§], Wei-Qi He[‡], Yan-Ning Qiao[‡], Ying-Ying Dong[‡], Yun-Qian Gao[‡], Chen Chen[‡], Cheng-Hai Zhang[‡], Wen Li[§], Hua-Hao Shen[§], Wen Ning[¶], Kristine E. Kamm[‖], James T. Stull[‖], Xiang Gao[‡], and Min-Sheng Zhu[‡1]

From the [‡]Model Animal Research Center of Nanjing University and MOE Key Lab of Model Animal for Disease Study, Nanjing 210061, China, the [§]Department of Respiratory Disease, Second Hospital of Medical School of Zhejiang University, Hangzhou 310009, China, the [¶]College of Life Science, Nankai University, Tianjin 300071, China, and the [‖]Department of Physiology, University of Texas Southwestern Medical Center, Dallas, Texas 75390

Different interacting signaling modules involving Ca^{2+}/calmodulin-dependent myosin light chain kinase, Ca^{2+}-independent regulatory light chain phosphorylation, myosin phosphatase inhibition, and actin filament-based proteins are proposed as specific cellular mechanisms involved in the regulation of smooth muscle contraction. However, the relative importance of specific modules is not well defined. By using tamoxifen-activated and smooth muscle-specific knock-out of myosin light chain kinase in mice, we analyzed its role in tonic airway smooth muscle contraction. Knock-out of the kinase in both tracheal and bronchial smooth muscle significantly reduced contraction and myosin phosphorylation responses to K^+-depolarization and acetylcholine. Kinase-deficient mice lacked bronchial constrictions in normal and asthmatic airways, whereas the asthmatic inflammation response was not affected. These results indicate that myosin light chain kinase acts as a central participant in the contractile signaling module of tonic smooth muscle. Importantly, contractile airway smooth muscles are necessary for physiological and asthmatic airway resistance.

Smooth muscles line the walls of hollow organs such as the airways of the respiratory tract. They are essential for maintaining homeostasis but also contribute to stress imposed by disease processes. Based on their different contractile properties, smooth muscle tissues from different organ systems are classified as phasic and tonic types. The typical phasic muscles (such as ileum, taenia coli, uterus, and portal vein) generate action potentials, shorten rapidly, and typically produce spontaneous contraction (1, 2). On the other hand, tonic smooth muscles (airway, vascular, and sphincter smooth muscles) do not generate action potentials and spontaneous contractions, and they maintain contractile force for prolonged periods of time (2). Phasic and tonic smooth muscles share some common regulatory signaling pathways centered on the molecular motor myosin as well as membrane properties associated with calcium handling and cell adhesion (3–7). As a common mechanism, smooth muscle contraction may be regulated by Ca^{2+} through two pathways initiated by depolarization and agonist, respectively. Depolarization of the cell membrane activates voltage-gated Ca^{2+} channels resulting in Ca^{2+} influx, whereas agonist stimulation generally activates GPCRs[2] leading to inositol 1,4,5-trisphosphate formation and Ca^{2+} release from the sarcoplasmic reticulum (8, 9). The increase in cytosolic Ca^{2+} leads to smooth muscle contraction through MLCK activation by Ca^{2+}/calmodulin and myosin RLC phosphorylation (9, 10). Additionally, activation of GPCRs leads to inactivation of MLCP by agonist-induced PKC and RhoA/ROCK activation (11–14). These inhibitory mechanisms thus enhance RLC phosphorylation and force development (Ca^{2+} sensitization).

Several other proposed regulatory mechanisms include RLC phosphorylation by Ca^{2+}-independent kinases (5, 15) that may act synergistically with Ca^{2+} sensitization leading to the proposal that MLCK is required only for the initial contraction, whereas the sustained contraction involves activities of Ca^{2+}-independent kinases with myosin light chain phosphatase inhibition. Additionally, activation of actin-associated thin filament proteins may play a role in smooth muscle contraction (16). Thus, it is crucial to elucidate the functional contributions of these different signaling modules to understand the integrated contraction of airway smooth muscle. In phasic smooth muscle, deletion of MLCK abolished K^+-induced contraction and significantly reduced GPCR-mediated contraction, thus indicating the central role of RLC phosphorylation by this Ca^{2+}-dependent kinase (17). In tonic smooth muscle such as airway smooth muscle, other regulatory elements including Ca^{2+} sensitization and Ca^{2+}-independent kinases may play primary roles in sustained force development (5, 15, 18, 19).

Although bronchial hyper-responsiveness is a component of asthma, the mechanisms underlying this excessive narrowing of the airways are unclear. An intrinsic change in airway smooth muscle may contribute and include increases in MLCK

* This work was supported, in whole or in part, by National Basic Research Program of China Grants 973 2009CB942602, 2005CB522501, 2007CB947100, and 2009CB522101, National Institutes of Health Grant HL26043, and National Natural Science Funding of China Grant 30570911.

[1] To whom correspondence should be addressed: 12 Xue-Fu Rd., Pukou District, Nanjing 210061, China. Tel.: 86-25-58641529; Fax: 86-25-58641500; E-mail: zhums@nju.edu.cn.

[2] The abbreviations used are: GPCR, G protein-coupled receptor; MLCK, myosin light chain kinase; RLC, regulatory light chain; MLCP, myosin light chain phosphatase; ROCK, Rho kinase; MYPT1, myosin targeting subunit of myosin light chain phosphatase; PKG, cGMP-dependent protein kinase; ACh, acetylcholine; HE, hematoxylin and eosin; PKC, protein kinase C; IL, interleukin.

content (20, 21), enhancement of Ca^{2+}-sensitization pathway (22, 23), Ca^{2+}-independent kinases (24, 25), and/or remodeling of the actin cytoskeleton (26).

We therefore deleted MLCK in adult tonic airway smooth muscle to address its biochemical importance in physiological contractions as well as its role in airway smooth muscle responsiveness in an animal model of asthma.

EXPERIMENTAL PROCEDURES

Generation of Floxed Mlck Mice and Tissue-specific Knock-out Mice ($MLCK^{SMKO}$)—To generate $MLCK^{SMKO}$ mice, $Mlck^{flox/flox}$ mice were crossed with SM-$CreER^{T2}$ (ki) mice expressing a tamoxifen-activated Cre recombinase under control of the SM22 promoter as previously described (17, 27). To purify $MLCK^{SMKO}$ from 129/B6 background, we backcrossed the mice to C57BL/6 for six generations. Female MLCK-deficient and littermate control mice ($Mlck^{flox/+}$; $SM\text{-}CreER^{T2}$) at 8–12 weeks of age were used for all experiments. Tamoxifen was injected intraperitoneally for five consecutive days at a dose of 1 mg/day as described (27). The tamoxifen (100 mg, Sigma, T5648) was dissolved in 0.5 ml of ethanol followed by 9.5 ml of sunflower oil at a concentration of 10 mg/ml and stored at −20 °C for up to 1 month. All experiments were conducted in accordance with the Animal Care and Use Committee of the Model Animal Research Center of Nanjing University.

Tracheal Contractility—Analysis of mouse tracheal contractility was performed as reported previously (28). Tracheae were excised and dissected free of surrounding tissues and cut into 2-mm length rings. The tracheal rings were opened and suspended on tissue hooks in individual 10-ml jacketed organ baths containing modified Krebs-Henseleit solution maintained at 37 °C, pH 7.4, gassed with a mixture of 95% O_2 and 5% CO_2 for a 30-min equilibration period. The Krebs-Henseleit solution consisted of the following composition: NaCl 118.1 mM, KCl 4.7 mM, $CaCl_2$ 2.5 mM, $MgSO_4$ 1.2 mM, KH_2PO_4 1.2 mM, $NaHCO_3$ 25 mM, glucose 11.1 mM. Force was recorded isometrically by a transducer (MLT0202, ADInstruments) connected to a PowerLab (ADInstruments) recording device. At the end of the equilibration period, KCl (60 mM) or acetylcholine (10 μM) were added to measure contractile responses. Acetylcholine was then applied cumulatively to obtain dose-dependent responses. Force per cross-sectional area was calculated from the tracheal muscle cross-sectional area obtained from histological images of each tissue.

Bronchial Ring Isometric Contraction Bioassay—Mouse bronchial ring contractility was measured as reported in detail (29). Briefly, the entire respiratory tree was rapidly removed from anesthetized mice and immersed in Krebs-Henseleit solution. Bronchial rings, 200–400 μm in diameter and 2 mm in length, were isolated from mouse intrapulmonary bronchi and mounted in a small-vessel wire myograph chamber (Danish Myo Technology, Aarhus, Denmark) by threading on two steel wires (40 μm in diameter) secured to two supports. One support was attached to a micrometer allowing control of ring circumference, whereas the other support was attached to a force transducer for measurements of isometric force development. The preparation was immersed in 6 ml of Krebs-Henseleit solution, bubbled with 95% O_2 and 5% CO_2, and maintained at 37 °C. Isometric force was initially set to 0 and the bronchial ring was allowed to equilibrate for 10 min. The bronchial ring was then stretched by applying a total of 7.5 millinewtons force (in 3 discrete steps of 2.5 millinewtons force with 5 min between intervals). After equilibration, KCl (60 mM) or acetylcholine (10 μM) were added to the bath, respectively, and the bronchial ring isometric force was recorded using a data acquisition and analysis program (Danish Myo Technology, Aarhus, Denmark).

Histopathology—Lungs were infused with 4% formalin through the tracheal cannula at a constant pressure of 25 cm of H_2O to inflation fix the lung. Specimens were immersed in 4% formalin overnight and dehydrated in a graded series of ethanol solutions. Tissue was embedded in paraffin. Sections were cut at 5 μm thickness and mounted onto positively charged slides (APES). Standard HE staining was performed. For quantification of bronchial smooth muscle, the thickness of the smooth muscle layer (the transverse diameter) was measured from the innermost edge to the outermost edge. The smooth muscle layer thickness was assessed at four predetermined bronchiole sites (12, 3, 6, and 9 o'clock) in at least 10 bronchioles of similar size (150–200 μm) on each slide (30). At the same time, smooth muscle nuclei were counted and normalized by mm^2 of muscle layer for trachea and by the length of the muscle layer for bronchioles.

Immunohistochemistry—Cryosections (10 μm) of lung and trachea were fixed in ice-cold acetone for 10 min and nonspecific binding of primary antibodies was blocked by incubation with phosphate-buffered saline containing 0.1% Triton X-100, 0.1% Tween 20, 1% BSA, and 5% non-immune goat serum for 1 h. Incubation was performed overnight with mouse monoclonal antibody to MLCK (K36, Sigma), diluted 1:100, together with a rabbit monoclonal α-smooth muscle actin antibody (clone 1A4, 1:100; Neomarkers). After washing in phosphate-buffered saline/Tween, the sections were incubated with a fluorescein isothiocyanate-conjugated goat anti-mouse antibody (Sigma) diluted 1:200 and a Alexa Fluor 555-conjugated goat anti-rabbit antibody (Invitrogen) diluted 1:100 for 1 h, and after a final wash step, the sections were mounted with phosphate-buffered glycerol, pH 7.4. Immunoreactivity was evaluated using a TCS-SP2 AOBS confocal laser scanning microscope (Leica, Heidelberg, Germany).

Western Blot Analysis—Western blot analyses were performed for measurement of MLCK and other protein expressions (31). Briefly, tissue samples were frozen quickly in 10% trichloroacetic acid and 10 mM dithiothreitol in acetone precooled to a slush at −80 °C. After homogenizing thoroughly, the sample pellet was washed three times with ether for 5 min each and dried to remove residual ether. The protein was dissolved completely in 8 M urea solution. Protein concentration was measured with a bicinchoinic acid protein assay reagent (Bio-Rad). Equal amounts of protein were loaded for SDS-PAGE followed by protein transfer to a nitrocellulose membrane. The membrane was then probed with a monoclonal antibody to MLCK (K36, Sigma) and secondary antibody sequentially. The membrane was incubated in Super Signal West Dura substrate (Pierce) before exposure to film. Antibodies for other proteins included integrin-linked protein kinase (Sigma), total MYPT1 (Upstate), phospho-MYPT1(Thr-696) (Upstate), phospho-MYPT1(Thr-850) (Upstate), ZIP kinase

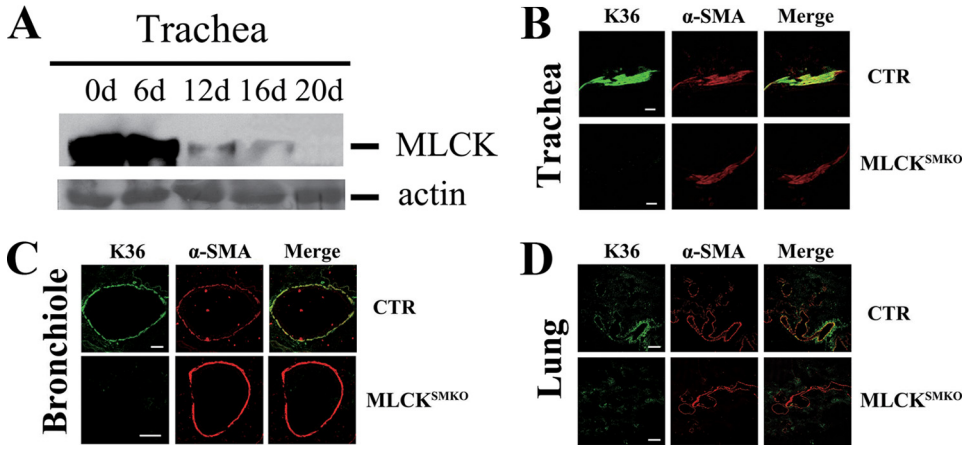

FIGURE 1. **Targeted disruption of the *Mlck* gene in airway smooth muscle.** *A*, Western blots of MLCK in tracheae from tamoxifen-treated mice collected at the indicated days (*d*) after treatment. Total actin stained with Coomassie Brilliant Blue G-250 was used as protein loading control. Immunofluorescence analysis of MLCK expression in tracheal (*B*) and lung (*C* and *D*) smooth muscle from control (*CTR*) and MLCK^{SMKO} mice. At the 16th day after tamoxifen injection, the trachea and lung of MLCK-deficient mice and control were embedded in OCT and sectioned. After acetone fixation, frozen sections were stained with K36 antibody and α-smooth muscle actin antibody. *Scale bars* in *panels B-D* are 80, 100, and 200 μm, respectively.

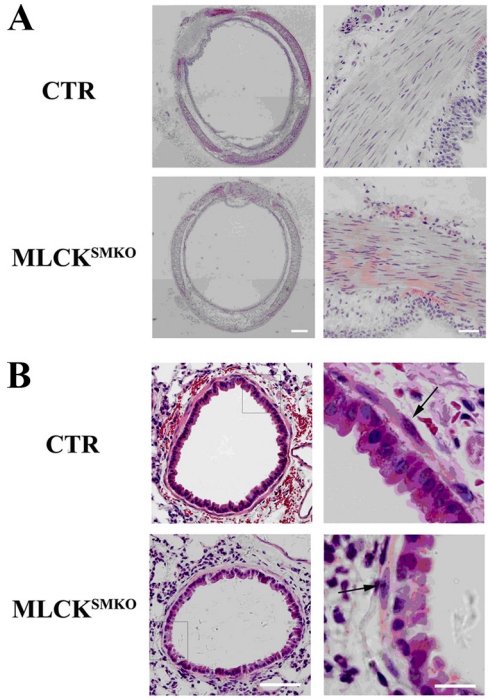

FIGURE 2. **Histological analysis of MLCK-deficient airway smooth muscle.** Fresh tracheal and lung tissues from control (*CTR*) and MLCK^{SMKO} knock-out mice were fixed with 4% formalin and dehydrated in a graded series of ethanol solutions followed by standard paraffin section and HE staining. Whole image of tracheal histology (*left part* of *panel A*) was made by merging images from different fields (marker measures 160 μm). Magnification for tracheal smooth muscle layer is shown in the *right part* of *panel A* (*scale bar* = 40 μm). *Panel B* represents histology of bronchiole in lung tissues (*scale bar* = 50 μm) and the magnification for the inset frame is shown in *right part* of *panel B* (*scale bar* = 15 μm). The *arrows* indicate smooth muscle cells.

(Sigma), ROCK II (Santa Cruz), sGC (Cayman Chemical), and PKG (Stressgen).

Measurement of Myosin Regulatory Light Chain Phosphorylation—Urea/glycerol-PAGE electrophoresis was used for measurement of RLC phosphorylation where the non-phosphorylated RLC is separated from the monophosphorylated RLC (31). Trachea were excised, dissected free of surrounding tissues, and then equilibrated for 30 min in the Krebs-Henseleit solution. The trachea were then incubated with 10 μM acetylcholine or 60 mM KCl for different times and transferred into 10% trichloroacetic acid and 10 mM dithiothreitol in acetone precooled at −80 °C to stop reactions. Tissues were homogenized, dissolved in sample buffer containing 8 M urea, 234 mM sucrose, 23 mM glycine, 10.4 mM dithiothreitol, 20 mM Tris, pH 8.6, and 0.01% bromphenol blue, and loaded into urea/glycerol-PAGE gels.

Immunization and Airway Challenge—Six- to eight-week-old female mice were sensitized to ovalbumin by intraperitoneal injection of 80 μg of OVA (Grade VI; Sigma) adsorbed to 4 mg of aluminum hydroxide (Pierce) in a total volume of 0.2 ml of sterile saline on days 0 and 14. These mice were then challenged for 60 min to aerosolized 1% ovalbumin by ultrasonic nebulization on days 24, 25, and 26. Sham-immunized animals received saline-diluted aluminum hydroxide intraperitoneal and aerosolized saline. From day 9 to 13, both MLCK^{SMKO} mice and control mice were injected with tamoxifen intraperitoneally at a dose of 1 mg/day.

Airway Responsiveness—Analysis of airway responsiveness to methacholine was performed as previously described (32). Briefly, on the day after the final aerosol challenge, airway responsiveness was measured noninvasively using a whole body plethysmograph (model PLY 3211, Buxco Electronics, Troy, NY). Pulmonary airflow obstruction was measured by use of the enhanced pause variable (Penh) according to the following formula: $Penh = [(Te/RT) - 1] \times (PEF/PIF)$, where $Penh$ = enhanced pause (dimensionless), Te = expiratory time, RT = relaxation time, PEF = peak expiratory flow (ml/s), and PIF = peak inspiratory flow (ml/s) (33). Penh is a calculated parameter that reflects changes in the waveform of the measured box pressure signal and thus, the shape of the respiratory cycle. The average Penh over 3 min was determined after a 2-min exposure to aerosolized normal saline as a baseline. Aerosolized methacholine in increasing concentrations were nebulized for 3 min and the average Penh over 3 min was then determined. Results were expressed as the percentage increase of Penh following challenge with each concentration of methacholine.

Whole Lung Lavage—Animals were injected intraperitoneally with a lethal dose of pentobarbital (450 mg/kg). The trachea was cannulated, and the lung was then lavaged with 0.8 ml of phosphate-buffered saline three times and the fluid pooled. Cells in the lavage fluid were counted using a hemocytometer, and BAL cell differentials were determined on slide preparations stained with hematoxylin and eosin. At least 200 cells were differentiated by light microscopy based on conventional

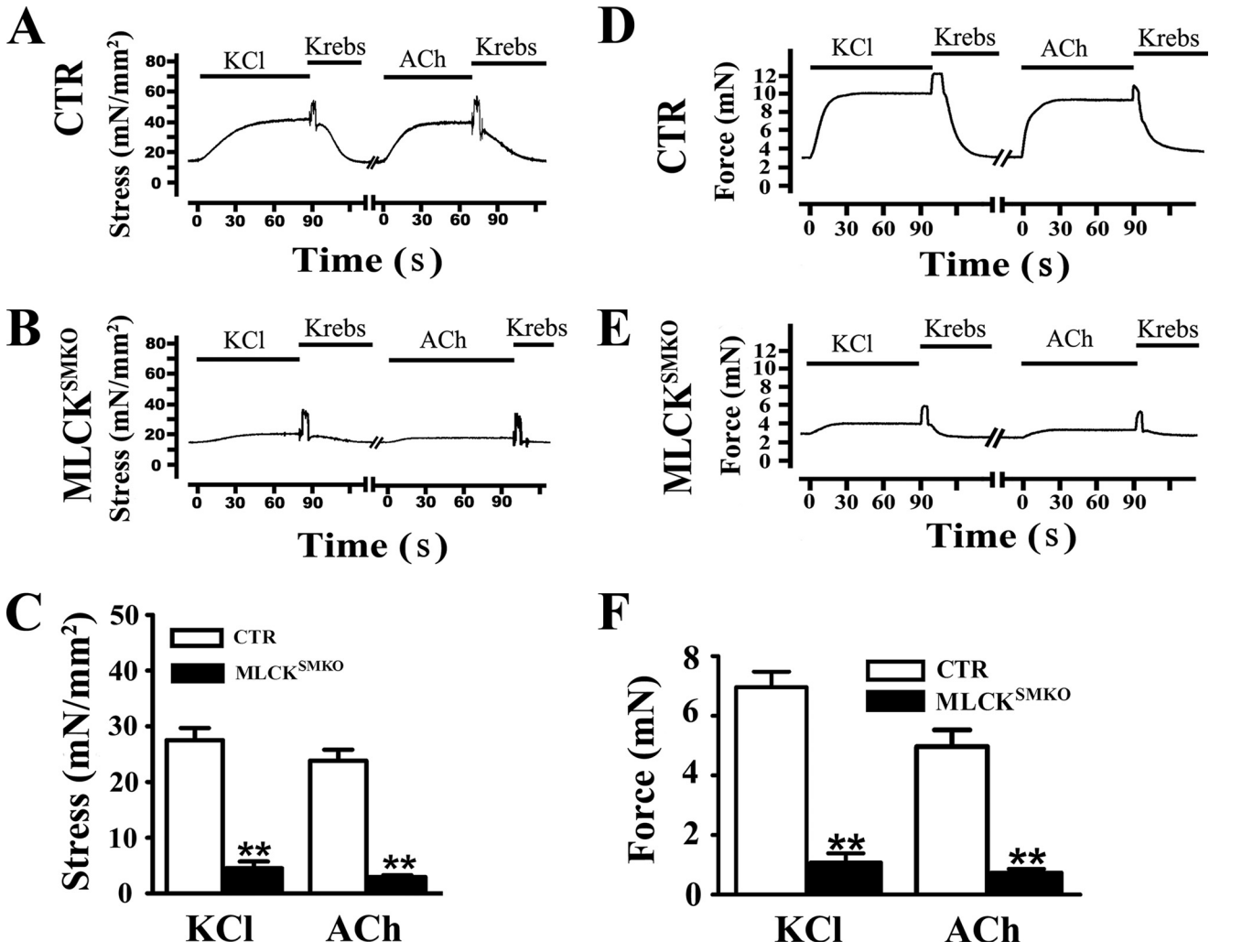

FIGURE 3. **Reduced contractions of tracheal and bronchial smooth muscle from MLCK^{SMKO} mice.** Representative recordings of tracheal ring contraction from control (*CTR*) (*A*) and MLCK^{SMKO} (*B*) mice treated with 60 mM KCl or 10 μM ACh. *Bars* show duration of stimulation. Quantification of contraction responses to KCl and ACh is summarized (*C*). *Columns* represent mean ± S.E., $n = 4–10$; **, $p < 0.01$. Representative recordings of bronchial ring contraction from CTR (*D*) and MLCK^{SMKO} (*E*) mice treated with 60 mM KCl or 10 μM ACh are shown. Quantification of bronchial contraction responses to KCl and ACh are shown (*F*). *Columns* represent mean ± S.E., $n = 4–6$; **, $p < 0.01$. *Error bars* indicate S.E.

morphologic criteria. The levels of cytokine IL-4, IL-5 in lavage fluid, and OVA-specific IgE in serum were determined using commercially available enzyme-linked immunosorbent assay kits (Aquatic Diagnostic Ltd. Biotechnology and Dev. Co.) as per the manufacturer's instructions.

Statistical Analysis—Data are presented as the mean ± S.E. Differences between groups were determined by Student's *t* test with significance at $p < 0.05$.

RESULTS

Ablation of MLCK Expression in Airway Smooth Muscle and Phenotypic Characterization of MLCK^{SMKO} Mice in C57BL/6 Background—A purified genetic background of knock-out mice may reduce phenotypic variation in normal animals and animal models of disease. Therefore we back-crossed (129:B6) MLCK^{SMKO} mice to C57BL/6 for six generations. Fig. 1*A* shows a representative time course for MLCK deletion in tracheal smooth muscle. At day 16 after starting the tamoxifen injections, only a small amount of MLCK protein was detected by Western blots, whereas almost no MLCK protein was typically detected by day 20. Immunohistochemistry with co-staining by anti-MLCK and anti-smooth muscle actin antibody confirmed the absence of MLCK in the trachea of MLCK^{SMKO} mice 16 days after tamoxifen injection (Fig. 1*B*). To examine MLCK expression in mutant bronchial smooth muscle, immunohistochemistry was performed on lung sections. The results also showed an absence of MLCK protein in bronchial and lung smooth muscle at 16 days after tamoxifen (Fig. 1, *C* and *D*). Thus, we conclude that MLCK^{SMKO} mice exhibit an efficient deletion of MLCK in airway smooth muscles.

Macrophenotypic analysis for MLCK^{SMKO} mice in the B6 background showed very similar characteristics to mixed background mice as described previously, except for a minor difference in the time course to death after treatment with tamoxifen (17). Mice in the B6 background died at 20 ± 1 days after tamoxifen treatment, whereas the original MLCK^{SMKO} mice died 17 days after induction. These different times appear consistent with the differences in MLCK protein deletion.

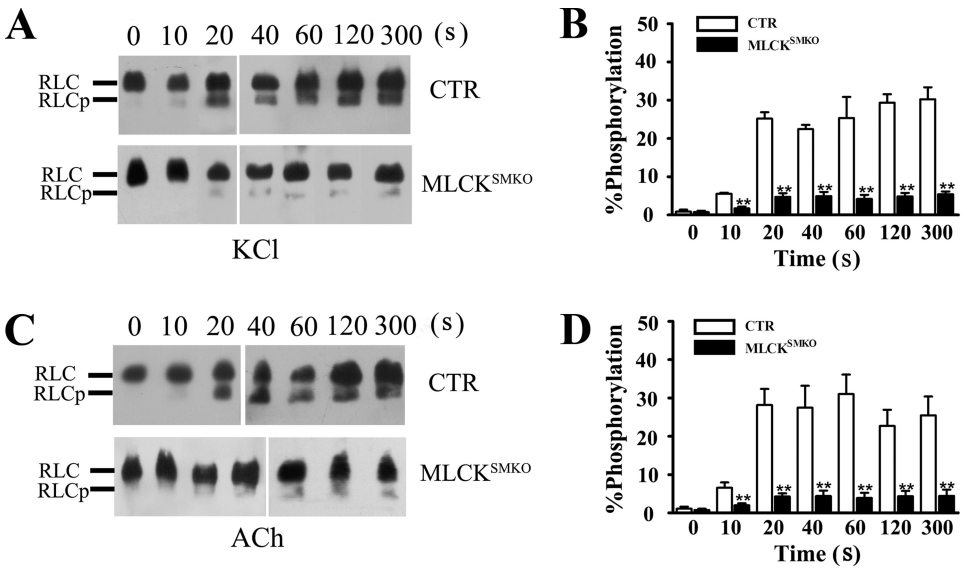

FIGURE 4. **Inhibition of RLC phosphorylation in tracheal smooth muscle from MLCK^{SMKO} mice.** RLC phosphorylation (*RLCp*) was measured in quick-frozen tracheal rings from control and MLCK^{SMKO} mice treated with 60 mM KCl (*A* and *B*) or 10 μM ACh (*C* and *D*) as shown by representative Western blots of glycerol/urea PAGE gels and quantification. *Columns* represent mean. *Error bars* indicate S.E., $n = 4–6$; **, $p < 0.01$.

Our previous analysis of gut smooth muscle showed a significant hypertrophy of smooth muscle cells in MLCK^{SMKO} mice (17). To determine whether the airway smooth muscle of MLCK^{SMKO} mice also displays hypertrophy, histological morphometry of tracheal and bronchial smooth muscle was performed. The mutant trachea exhibited a comparable histological morphology relative to control trachea, and no hypertrophy was apparent by measuring the thickness of the muscle layer (157 ± 24 *versus* 160 ± 17 μm from control mice, $p > 0.05$; $n =$ 5 sections from 3 mice) or number of nuclei per mm^2 of smooth muscle (2885 ± 151 *versus* 2823 ± 166, $p > 0.05$) (Fig. 2*A*). Similarly, bronchial smooth muscle thickness was comparable (5.14 ± 0.37 μm for control mice *versus* 5.03 ± 0.35 μm for MLCK^{SMKO}, $p > 0.05$; $n = 7$ sections from 3 mice) with a comparable number of cell nuclei per millimeter of muscle layer (41 ± 7 *versus* 43 ± 6 for control mice, $p > 0.05$) (Fig. 2*B*). Thus, MLCK deletion in airway smooth muscle did not affect morphological properties.

Reduced Contraction of MLCK-deficient Airway Smooth Muscle—To determine the contractile properties of MLCK-deficient airway smooth muscle, we measured force development by tracheal and bronchial smooth muscles in response to KCl and muscarinic agonists and calculated stress values (force normalized to tissue cross-sectional area). Tracheal rings isolated from MLCK-deficient mice developed an average 16.4% of the stress relative to control tissues in response to 60 mM KCl (Fig. 3, *A–C*). The responses to KCl with and without the muscarinic antagonist atropine were similar (data not shown), indicating that KCl did not stimulate ACh release from parasympathetic nerve endings in tracheal tissues. Tracheal smooth muscle from MLCK-deleted mice displayed 12.4% stress responses to 10 μM ACh compared with control muscles (Fig. 3, *A–C*). Treatment with atropine abolished the ACh-induced contraction in smooth muscles, indicating a muscarinic-specific response (data not shown). These results clearly show that deletion of MLCK results in a significant reduction in responses to K^+ depolarization and muscarinic receptor activation in tracheal smooth muscle.

Bronchial smooth muscle distributes evenly around the bronchus, and is important for producing airway resistance. We measured the contractile responses of bronchial rings in response to KCl and ACh. Greater force responses were obtained in bronchial rings from control mice *versus* MLCK-deficient mice in response to KCl (Fig. 3, *D–F*). Bronchial smooth muscles from knock-out mice displayed only 15% force relative to control bronchioles. Similarly, the bronchial smooth muscle rings from MLCK^{SMKO} mice developed only 15% of the stresses developed by control tissue in response to ACh (Fig. 3, *D–F*). Thus, MLCK depletion also leads to impairment of bronchial smooth muscle contraction in response to KCl and agonist. Due to similar contractile responses of trachea and bronchial smooth muscles, we used tracheal smooth muscle for subsequent biochemical analyses.

RLC Phosphorylation Responses Are Inhibited in MLCK^{SMKO} Tracheal Smooth Muscles—Our previous results showed that MLCK-catalyzed myosin light chain phosphorylation is required for phasic smooth muscle contraction (17). To assess the functional contribution of MLCK-mediated RLC phosphorylation in tonic contraction of tracheal smooth muscle, we measured RLC phosphorylation in response to KCl and ACh. In control tracheal muscle, RLC phosphorylation increased from a resting value of 1.1 to 25.2% by 20 s after KCl stimulation and then remained elevated; in MLCK-deficient tracheal muscle, RLC phosphorylation increased from 0.8% to only 5.0% after KCl stimulation (Fig. 4, *A* and *B*). With ACh-induced contraction, RLC phosphorylation increased to 28.0% at 20 s in control tracheal tissues (Fig. 4, *C* and *D*). In MLCK^{SMKO} trachea, however, RLC was phosphorylated to only 4.3% by 20 s after ACh stimulation. No diphosphorylated RLC was detected in mutant or control trachaea. Importantly, there were no additional increases in RLC phosphorylation with a contraction sustained for up to 300 s (Fig. 4, *C* and *D*). These results are consistent with the marked attenuation of force development in tracheal muscles from MLCK^{SMKO} mice by KCl and agonist stimulation. Thus, MLCK appears to be the primary kinase that phosphorylates RLC in response to both K^+ depolarization and muscarinic receptor activation. These results show that MLCK-mediated RLC phosphorylation is important for both the initial and sustained contractile responses of airway smooth muscle.

The Residual Contraction of MLCK-deleted Trachea Is Calcium-dependent and Blebbistatin-sensitive, but Less Sensitive to Acetylcholine—There were small contractile and RLC phosphorylation responses to KCl and agonists in MLCK-deficient airway smooth muscle. To understand the production of resid-

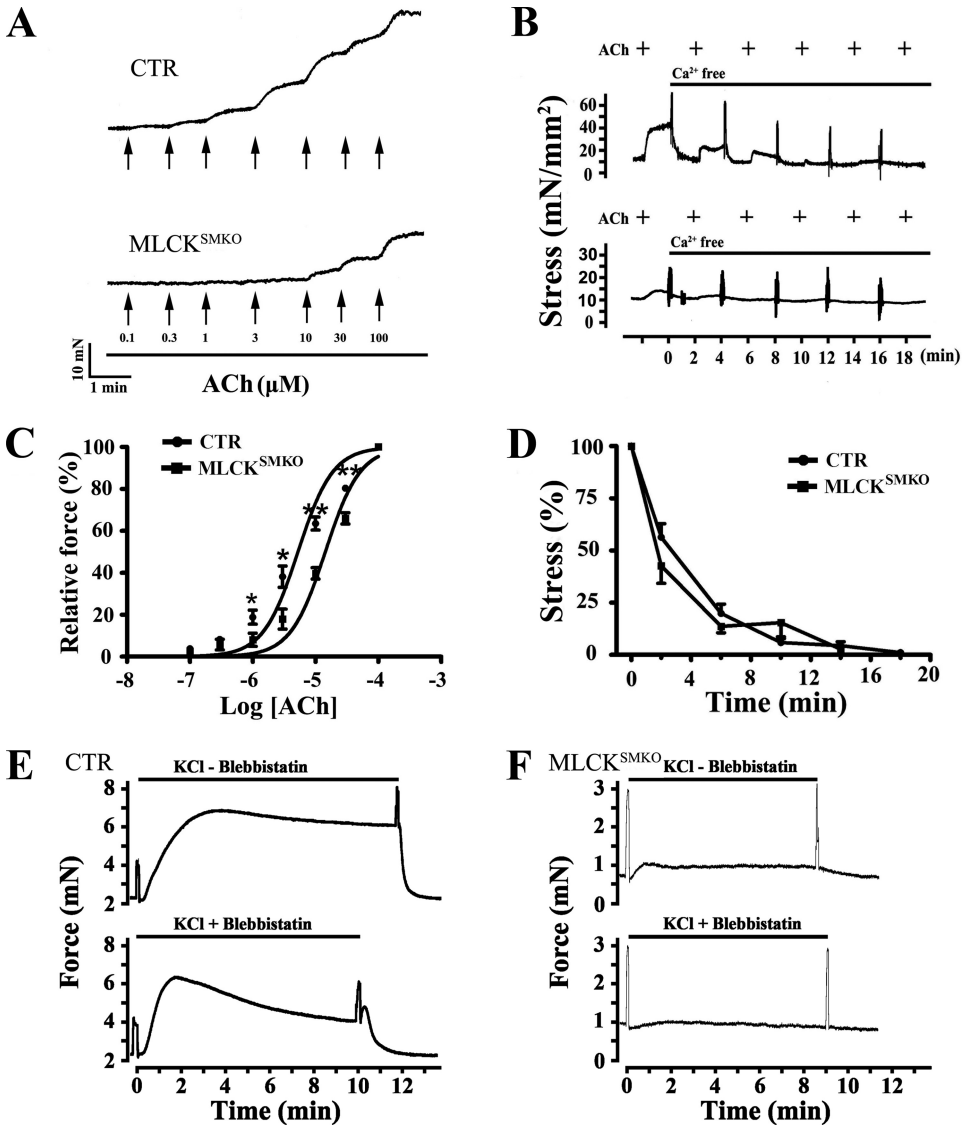

FIGURE 5. **Ca^{2+} dependence of small contractions of MLCK-deficient trachea.** Sensitivity to ACh of MLCK-deficient and control (*CTR*) trachea was assessed by isometric force measurements in response to cumulative increases in the concentration of ACh (*A*), and expressed as percent of maximal force with ACh (*C*). *Arrows* indicate the point at which the concentration of acetylcholine was increased; mean ± S.E. from 7 control (*CTR*) and 5 $MLCK^{SMKO}$ tracheal rings are shown; *, $p < 0.05$; **, $p < 0.01$. *Panels B* and *D* show the effects of Ca^{2+} depletion on tracheal smooth muscle contraction. Depletion of Ca^{2+} in CTR and $MLCK^{SMKO}$ tracheal smooth muscle by adding 1 mM EGTA in the bath solution inhibited the contractile responses to repeated exposure to 10 μM ACh (*B*). Quantification of contractile responses by CTR and $MLCK^{SMKO}$ muscles with Ca^{2+} depletion and normalized to pre-treatment values (*D*). Values are mean ± S.E. ($n = 3–4$). *Panels E* and *F* represent a typical inhibitory effect of blebbistatin on tracheal smooth muscle contraction. With or without addition of 30 μM blebbistatin to the incubation buffer, the isometric force of control (*E*) and MLCK-deficient (*F*) trachea developed with 80 mM KCl was measured. Each measurement was repeated in three to five independent animals.

ual contraction, we determined the properties in terms of sensitivity to ACh and dependence on calcium. As the concentration of ACh cumulatively increased up to 3 μM, MLCK-deficient tracheal smooth muscle started to contract, reaching a maximum response at 100 μM. In contrast, trachaea from control animals started to contract at 0.1 μM ACh, developing a maximum contractile response at 10 μM (Fig. 5, *A* and *C*). The EC_{50} values for ACh were 5.4 ± 2.8 (control; $n = 7$) and 14.5 ± 3.3 μM ($MLCK^{SMKO}$; $n = 5$), respectively, showing that tracheal smooth muscles from $MLCK^{SMKO}$ mice have significantly lower sensitivity to ACh ($p < 0.01$).

To determine whether the small contraction of MLCK-deleted tracheal muscle is Ca^{2+}-dependent, we depleted intracellular Ca^{2+} by repeated ACh applications in the presence of EGTA. Results showed that Ca^{2+} depletion inhibited the robust contractile response in control trachea as well as the smaller contraction in $MLCK^{SMKO}$ trachea (Fig. 5, *B* and *D*). Thus, the small contraction induced by ACh in $MLCK^{SMKO}$ tonic muscle is Ca^{2+} dependent.

We also determined the inhibitory effect of the selective myosin II inhibitor blebbistatin (34, 35). Results showed that addition of 30 μM blebbistatin inhibited both the robust (KO, 34 ± 18%, $n = 3$; CTR, 14 ± 8%, $n = 5$) and sustained (KO, 81 ± 10%, $n = 3$; CTR, 37%, $n = 5$) contractile response to KCl in the $MLCK^{SMKO}$ trachea as well as control trachea (Fig. 5, *E* and *F*). The higher percent inhibition in mutant trachea might be due to the smaller amount of force or the atypical contraction waveform. Thus, the small contraction in $MLCK^{SMKO}$ tonic muscle is sensitive to blebbistatin.

Normal cGMP/PKG and RhoA/ROCK Signaling in Trachea from $MLCK^{SMKO}$ Mice—Reduced contractile responses may be contributed by decreased Rho/ROCK signaling or by increased cGMP/PKG signaling (5). To rule out possible compensatory effects during the contraction response of MLCK-deleted trachea, we measured relative amounts of key proteins in these signaling modules (17, 36). Compared with control muscle, the knock-out trachea smooth muscle had comparable expression levels of integrin-linked protein kinase, ROCK II, MYPT1, and ZIP kinase (Fig. 6*A*). Phosphorylation responses for MYPT1 (MYPT1-p696 and MYPT1-p850) to agonist were not altered in MLCK-deficient tracheae compared with controls (Fig. 6*B*). cGMP/PKG signaling may affect smooth muscle contraction so we measured sGC and PKG amounts (31). Results showed a comparable expression of sGC and PKG in the trachea from the knock-out *versus* control mice (Fig. 6*C*). These observations indicate normal amounts of key proteins involved in the cGMP/PKG and RhoA/ROCK pathways in tracheae from $MLCK^{SMKO}$ mice.

Deletion of MLCK Abolished Physiological and Asthmatic Bronchial Constriction—To assess the effect of MLCK deletion on the respiratory system under physiological conditions, we measured airway constriction and other respiratory parameters in a whole body plethysmograph with inhalation of increasing amounts of the muscarinic agonist, methacholine. MLCK^{SMKO} mice appeared to exhibit less change in airway resistance as estimated by the enhanced pause variable (Penh) compared with control mice ($p < 0.01$) (Fig. 7*A*). The time of inspiration of knock-out mice was reduced significantly ($p < 0.05$) and the minute volume became larger (Fig. 7, *B* and *E*). The time of expiration and tidal volume showed no significant difference ($p > 0.05$) (Fig. 7, *C* and *D*).

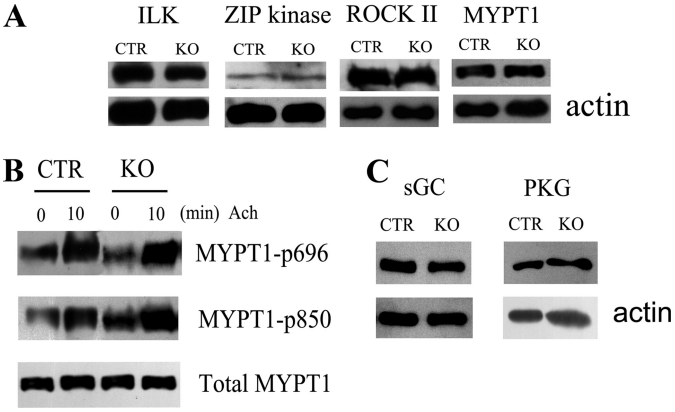

FIGURE 6. **Expression of contractile and related regulatory proteins in tracheae from MLCK^{SMKO} mice.** *A*, Western blots for integrin-linked protein kinase, ZIP kinase, ROCK II, and MYPT-1 expression in tracheal tissues from control (*CTR*) and MLCK^{SMKO} mice. The samples were resolved by separate SDS-PAGE and β-actin was stained with anti-actin antibody as a loading control. *B*, MYPT1 phosphorylation at residues 696 and 850 in response to 10 μM ACh were measured by anti-MYPT1-P696 and anti-MYPT1-P850 antibodies. *C*, Western blots for PKG and sGC expression in CTR and mutant tracheal tissues. Blots shown are representative of at least three measurements. *KO*, knock-out.

To determine whether the absence of MLCK activity protected against the development of asthmatic airway constriction associated with allergen-induced airway hyper-reactivity, MLCK^{SMKO} mice were sensitized to ovalbumin and then challenged with aerosol ovalbumin. Airway hyper-reactivity was then assessed by measurements of respiratory parameters as above. Whereas the ovalbumin-immunized control mice demonstrated robust airway hyper-reactivity, exhibited by much stronger airway constriction than non-immunized control mice, ovalbumin-immunized MLCK^{SMKO} mice showed no signs of airway hyper-reactivity ($p > 0.05$), even when challenged with a high concentration of methacholine (Fig. 7*A*). Taken together, our results show that deletion of MLCK abolishes airway constriction under both physiological and asthmatic conditions.

Deletion of MLCK Does Not Affect Allergic Inflammation in Asthmatic Airway—To determine whether the abolishment of airway constriction is caused by a failure of allergic sensitization, and whether the reduced constriction affects inflammation intensity, we examined lungs histologically and measured profiles of inflammatory cells and cytokines in lungs from control and MLCK^{SMKO} mice. Following sensitization and challenge with ovalbumin, both control and MLCK^{SMKO} mice showed significant inflammation in lung tissue with dense peribronchiolar and perivascular infiltrates consisting of lymphocytes, eosinophils, and neutrophils (Figs. 8 and 9*A*). Quantification for cellular composition shows about 30% eosinophils in bronchoalveolar fluid from both asthmatic control and MLCK^{SMKO} mice, suggesting a typical pattern of asthmatic inflammation cells. In contrast to non-sensitized mice, the sensitized mice exhibited significantly higher levels of ovalbumin-specific IgE, IL-4, and IL-5 (Fig. 9, *B* and *C*), showing a typical immune response of asthmatic inflammation. No differences were observed between knock-out and control groups ($p > 0.05$). In conclusion, our results show that the allergic

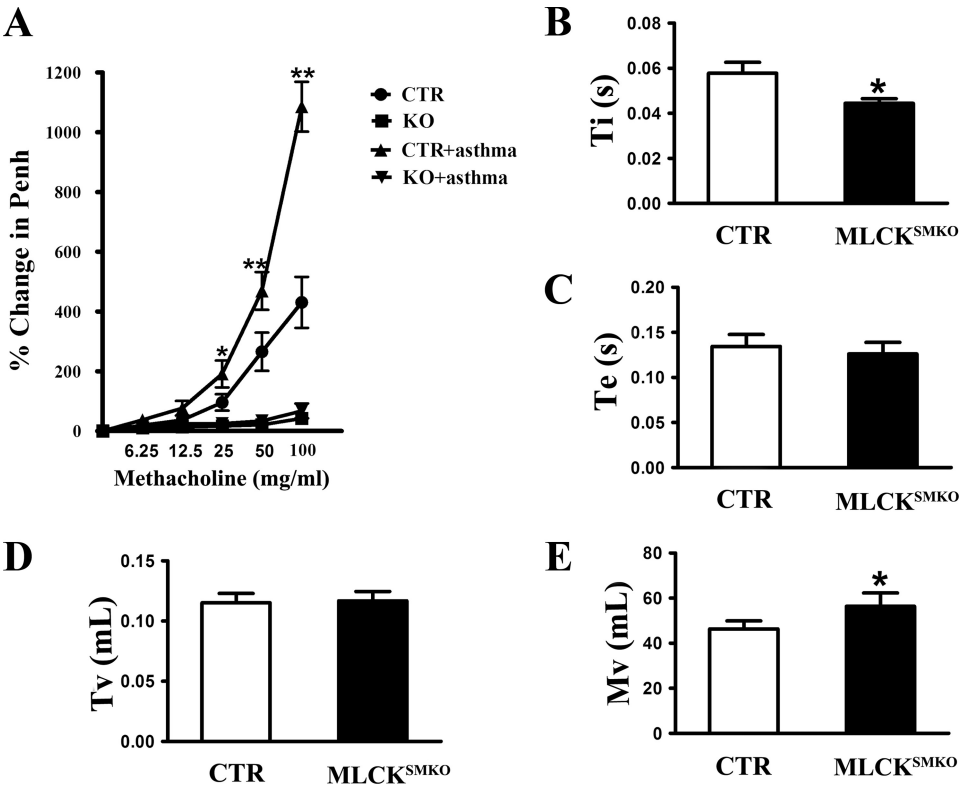

FIGURE 7. **Decreased airway respiratory resistance and altered breathing pattern in MLCK-deficient mice.** *A*, MLCK^{SMKO} and control (*CTR*) mice were immunized and challenged by OVA. On the day after the final aerosol challenge, airway responsiveness was measured noninvasively using whole body plethysmography. Data are expressed as percent above baseline. At the same time, some respiratory parameters such as Ti (*B*), Te (*C*), Tv (*D*), and Mv (*E*) at baseline were analyzed to compare the differences between the MLCK^{SMKO} and control mice. *Ti*, time of inspiration; *Te*, time of expiration; *Tv*, tidal volume; *Mv*, minute volume. Values are mean ± S.E. ($n = 6$). *Error bars* indicate S.E. *, $p < 0.05$; **, $p < 0.01$, as compared with same condition without asthma.

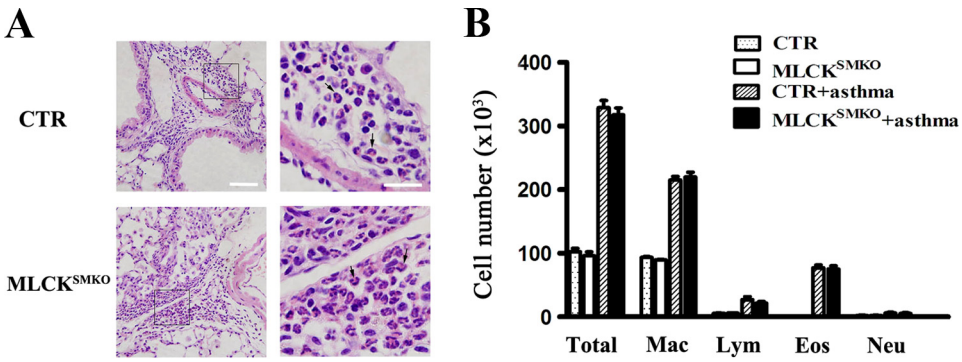

FIGURE 8. **Histopathology and inflammatory cells of lungs from control (*CTR*) and MLCK^{SMKO} mice sensitized to ovalbumin.** Two days after the last challenge with ovalbumin, the mice were anesthetized and killed. The lung and the bronchoalveolar fluid from mice were collected. *A*, histological examination (hematoxylin and eosin (HE) staining) of lung tissue from CTR mice (*upper panels*) shows dense perivascular and peribronchiolar eosinophils as indicated by the *arrows*. *Lower panels* show the histology of the lung from MLCK^{SMKO} mice. The mutant lung shows similar histopathologic changes. *Scale bar* in the *left panels* is 60 μm; *scale bar* in the *right panels* is 20 μm. *B*, total number of macrophages, eosinophils, lymphocytes, and neutrophils in the bronchoalveolar fluid were determined by counting HE-stained cells. *Dotted bars*, CTR/saline; *white bars*, MLCK^{SMKO}/saline; *hatched bars*, CTR/ovalbumin; *black bars*, MLCK^{SMKO}/ovalbumin. *Eos*, eosinophils; *Lym*, lymphocytes; *Mac*, macrophages; *Neu*, neutrophils. Values are mean (*columns*) ± S.E. (*error bars*) ($n = 6$).

inflammation of the asthmatic airway is similar in control and MLCK-deficient mice.

DISCUSSION

Ca^{2+}/calmodulin-dependent MLCK was originally proposed as an essential initiator of smooth muscle contraction because of its phosphorylation of RLC-activated myosin (10, 37). A simple cascade of biochemical reactions starting with Ca^{2+} binding to calmodulin, activation of MLCK, RLC phosphorylation, and force development for smooth muscle contraction was developed. A decrease in $[Ca^{2+}]_i$ and inactivation of MLCK allows RLC dephosphorylation and relaxation. However, more elaborate signaling modules involving regulation of MLCP activity emerged with additional studies. GPCR activation of RhoA leads to phosphorylation of the regulatory subunit of MLCP, MYPT1, by Ca^{2+}-independent kinases leading to inhibition of its phosphatase activity (5–7, 22). CPI-17 phosphorylated by PKC may also inhibit MLCP activity. Additionally, Ca^{2+}-independent kinases have been proposed to phosphorylate RLC directly. The relative physiological importance of these different signaling proteins is difficult to appreciate. Genetic approaches offer tools to unravel complexities in defining signaling modules in physiological responses and pathophysiological developments. We have thus used a conditional knock-out of MLCK in adult smooth muscle to define its function in airway physiology and pathological airway constrictions associated with asthma.

MLCK appears to play a central role in smooth muscle contractile responses. MLCK is clearly important in phasic smooth muscle contraction because its deletion significantly impairs transient force development and RLC phosphorylation (17). RLC phosphorylation and force are sustained in tonic smooth muscle contractions such as the airway smooth muscle (7, 38). Many studies suggest that the sustained RLC phosphorylation may be due to contributions from other imposing signaling pathways involving primarily inhibition of MLCP by activation of PKC and RhoA/ROCK pathways (7, 12–14) but also Ca^{2+}/CaM-independent kinases that act on both RLC and MLCP (5, 7, 19). Biochemical measurements show lower activities of MLCK and MLCP in tonic smooth muscles, with greater amounts of proteins in the RhoA/ROCK signaling module that could inhibit MLCP activity compared with phasic smooth muscle (39, 40). Others predict a potentially important role of Ca^{2+}-independent regulation acting directly to phosphorylate RLC (5, 7, 11, 15, 41). However, we find that deletion of Ca^{2+}/calmodulin-dependent MLCK in tonic airway smooth muscle greatly attenuated RLC phosphorylation as well as force development initially and during the sustained contraction phase with both depolarization and muscarinic receptor-induced contraction. Thus, MLCK and its phosphorylation of RLC play an essential role in airway smooth muscle contraction and most likely other tonic smooth muscles. Furthermore, inhibition of MLCP by phosphorylation of its regulatory subunit MYPT1 by itself appears insufficient for robust RLC phosphorylation and force development without MLCK activity. However, whereas these studies indicate that MLCK plays a central role as the kinase that directly phosphorylates RLC, the results do not diminish the documented important role for inhibition of myosin phosphatase activity in promoting Ca^{2+} sensitization.

Our results do not exclude the importance of MYPT1 phosphorylation in regulating MLCP activity during a contraction, because the function of MLCP will be dependent on RLC phosphorylation catalyzed by MLCK. Ca^{2+} dependence of the residual force developed by airway smooth muscle after MLCK gene ablation may be related to residual MLCK in which only a small fraction is necessary for sufficient RLC phosphorylation (31). Importantly, we could not find evidence that Ca^{2+}-independent kinase activity toward direct phosphorylation of RLC is involved in sustained contractions.

We examined the inhibitory effect of blebbistatin on MLCK-KO muscle, and found that the small contraction could be inhibited. Due to the small amount of force for residual contraction and atypical waveform of contraction, we could not determine whether the small contraction was more sensitive to blebbistatin, thereby indicating a primary contribution of non-muscle myosin II. However, we expect that MLCK also catalyzes non-muscle myosin phosphorylation if it contributes to force development in tonic contraction (42). Blebbistatin is an effective inhibitor of smooth muscle actomyosin and smooth muscle contraction from mammals and chicken arteries, whereas it is not as effective for inhibiting gizzard smooth muscle contractions, consistent with the original report that blebbistatin was not effective in inhibiting avian gizzard actomyosin ATPase activity (34).

The importance of MLCK in airway smooth muscle function is strongly supported by the phenotypes from measurements of airway respiratory resistance in knock-out mice where smooth

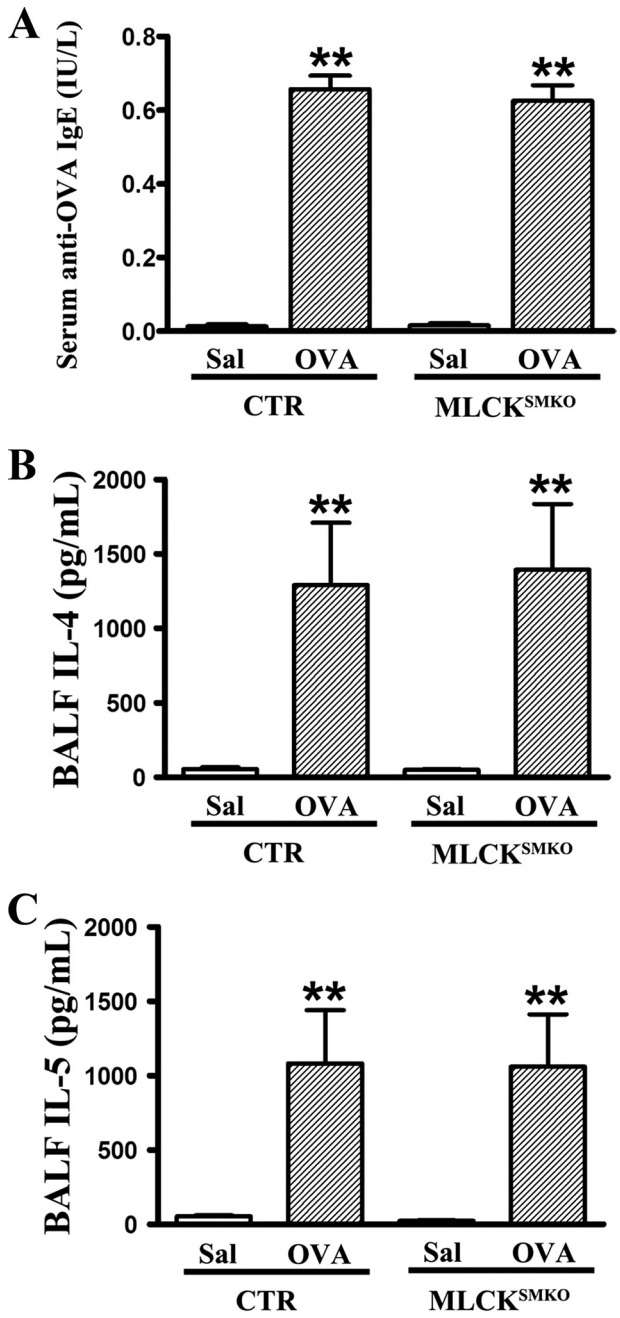

FIGURE 9. **Immunological responses of ovalbumin-sensitized control (*CTR*) and MLCK^{SMKO} mice.** After the last challenge with ovalbumin, bronchoalveolar fluids of mice were collected. Ovalbumin (*OVA*)-specific IgE in serum (*A*) and cytokines IL-4 (*B*) and IL-5 (*C*) in bronchoalveolar fluid were measured by enzyme-linked immunosorbent assay according to the manufacturer's instructions. Values are mean (*columns*) ± S.E. (*error bars*) ($n = 6$). **, $p < 0.01$.

muscle appears critical for airway constriction. Many external signals can invoke airway smooth muscle contraction through different signaling modules in which MLCK may serve as thw focal point, and hence control airway constriction (43). The loss-of-function evidence resulting from deletion of MLCK that caused almost complete abolishment of both physiological and asthmatic airway constriction clearly defines an essential role of MLCK in airway contraction. Moreover, as the knock-out mice displayed an alteration in breathing pattern with shorter inspirations and larger minute volumes compared with measurements from control mice, it appears that MLCK-mediated airway smooth muscle contraction could influence the breathing pattern as effectors of the pulmonary stretch reflex (44). Thus, relaxed airway smooth muscle may lead to reduced respiratory resistance and hence a quicker inspiration; however, the air in the lung is not dispelled efficiently without contraction, resulting in a larger minute volume. Therefore, we propose that airway smooth muscle regulates airflow turnover in a physiological breath by controlling air resistance.

Asthma is a disease characterized by chronic airway inflammation, airway hyper-reactivity, and airway remodeling, resulting in high airway constriction and episodic airway obstruction (45). The excessive contraction of airway smooth muscle is a primary contributing determinant for asthmatic airway constriction along with airway inflammation (46). Current treatments for asthma involving cholinergic, histaminergic, and leukotriene antagonists as well as anti-immune modulation and anti-inflammation approaches have provided limited successes and thus, asthma therapeutics continues to be an important area of clinical investigation (47). As asthma is accompanied by abnormal airway smooth muscle contraction in response to a wide variety of excitatory stimuli, specific inhibition of MLCK represents a potential therapeutic approach to treating symptoms.

Acknowledgments—We thank Dr. Xu Jun of Guangzhou Respiration Institute for providing technical assistance and valuable suggestions. We thank Dr. Robert Feil of Interfakultäres Institut für Biochemie (IFIB) Signaltransduktion for providing the SM-CreER(T2) mice.

REFERENCES

1. Golenhofen, K., and Mandrek, K. (1991) *Dig. Dis.* **9,** 341–346
2. Somlyo, A. V., and Somlyo, A. P. (1968) *J. Pharmacol. Exp. Ther.* **159,** 129–145
3. Ito, M., Nakano, T., Erdodi, F., and Hartshorne, D. J. (2004) *Mol. Cell. Biochem.* **259,** 197–209
4. Kamm, K. E., and Stull, J. T. (2001) *J. Biol. Chem.* **276,** 4527–4530
5. Murthy, K. S. (2006) *Annu. Rev. Physiol.* **68,** 345–374
6. Somlyo, A. P., and Somlyo, A. V. (1994) *Nature* **372,** 231–236
7. Somlyo, A. P., and Somlyo, A. V. (2003) *Physiol. Rev.* **83,** 1325–1358
8. Linder, M. E., and Gilman, A. G. (1992) *Sci. Am.* **267,** 56–61
9. Barnes, P. J., Rodger, I. W., and Thomson, N. C. (1992) *Airway Smooth Muscle*, pp. 59–84, Academic Press, London
10. Kamm, K. E., and Stull, J. T. (1985) *Annu. Rev. Pharmacol. Toxicol.* **25,** 593–620
11. Swärd, K., Mita, M., Wilson, D. P., Deng, J. T., Susnjar, M., and Walsh, M. P. (2003) *Curr. Hypertens. Rep.* **5,** 66–72
12. Dimopoulos, G. J., Semba, S., Kitazawa, K., Eto, M., and Kitazawa, T. (2007) *Circ. Res.* **100,** 121–129
13. Seko, T., Ito, M., Kureishi, Y., Okamoto, R., Moriki, N., Onishi, K., Isaka, N., Hartshorne, D. J., and Nakano, T. (2003) *Circ. Res.* **92,** 411–418
14. Khromov, A., Choudhury, N., Stevenson, A. S., Somlyo, A. V., and Eto, M. (2009) *J. Biol. Chem.* **284,** 21569–21579
15. Ihara, E., and MacDonald, J. A. (2007) *Can. J. Physiol. Pharmacol.* **85,** 79–87
16. Winder, S. J., and Walsh, M. P. (1993) *Cell Signal.* **5,** 677–686
17. He, W. Q., Peng, Y. J., Zhang, W. C., Lv, N., Tang, J., Chen, C., Zhang, C. H., Gao, S., Chen, H. Q., Zhi, G., Feil, R., Kamm, K. E., Stull, J. T., Gao, X., and Zhu, M. S. (2008) *Gastroenterology* **135,** 610–620
18. Harnett, K. M., Cao, W., and Biancani, P. (2005) *Am. J. Physiol. Gastrointest. Liver Physiol.* **288,** G407–G416

19. Somlyo, A. P., and Somlyo, A. V. (2004) *J. Muscle Res. Cell Motil.* **25,** 613–615
20. Jiang, H., Rao, K., Halayko, A. J., Liu, X., and Stephens, N. L. (1992) *Am. J. Respir. Cell Mol. Biol.* **7,** 567–573
21. Ammit, A. J., Armour, C. L., and Black, J. L. (2000) *Am. J. Respir. Crit. Care Med.* **161,** 257–263
22. Kume, H. (2008) *Curr. Med. Chem.* **15,** 2876–2885
23. Schaafsma, D., Gosens, R., Bos, I. S., Meurs, H., Zaagsma, J., and Nelemans, S. A. (2004) *Br. J. Pharmacol.* **143,** 477–484
24. Haystead, T. A. (2005) *Cell. Signal.* **17,** 1313–1322
25. Wu, Y., Huang, Y., Herring, B. P., and Gunst, S. J. (2008) *Am. J. Physiol. Lung Cell Mol. Physiol.* **295,** L988–L997
26. Kim, H. R., Appel, S., Vetterkind, S., Gangopadhyay, S. S., and Morgan, K. G. (2008) *J. Cell Mol. Med.* **12,** 2165–2180
27. Kühbandner, S., Brummer, S., Metzger, D., Chambon, P., Hofmann, F., and Feil, R. (2000) *Genesis* **28,** 15–22
28. McGraw, D. W., Almoosa, K. F., Paul, R. J., Kobilka, B. K., and Liggett, S. B. (2003) *J. Clin. Invest.* **112,** 619–626
29. Liu, J. Q., Yang, D., and Folz, R. J. (2006) *Am. J. Physiol. Lung Cell Mol. Physiol.* **291,** L281–L288
30. Cho, J. Y., Miller, M., Baek, K. J., Han, J. W., Nayar, J., Lee, S. Y., McElwain, K., McElwain, S., Friedman, S., and Broide, D. H. (2004) *J. Clin. Invest.* **113,** 551–560
31. Isotani, E., Zhi, G., Lau, K. S., Huang, J., Mizuno, Y., Persechini, A., Geguchadze, R., Kamm, K. E., and Stull, J. T. (2004) *Proc. Natl. Acad. Sci. U.S.A.* **101,** 6279–6284
32. Hansen, G., Jin, S., Umetsu, D. T., and Conti, M. (2000) *Proc. Natl. Acad. Sci. U.S.A.* **97,** 6751–6756
33. Hamelmann, E., Schwarze, J., Takeda, K., Oshiba, A., Larsen, G. L., Irvin, C. G., and Gelfand, E. W. (1997) *Am. J. Respir. Crit. Care Med.* **156,** 766–775
34. Eddinger, T. J., Meer, D. P., Miner, A. S., Meehl, J., Rovner, A. S., and Ratz, P. H. (2007) *J. Pharmacol. Exp. Ther.* **320,** 865–870
35. Straight, A. F., Cheung, A., Limouze, J., Chen, I., Westwood, N. J., Sellers, J. R., and Mitchison, T. J. (2003) *Science* **299,** 1743–1747
36. Sausbier, M., Zhou, X. B., Beier, C., Sausbier, U., Wolpers, D., Maget, S., Martin, C., Dietrich, A., Ressmeyer, A. R., Renz, H., Schlossmann, J., Hofmann, F., Neuhuber, W., Gudermann, T., Uhlig, S., Korth, M., and Ruth, P. (2007) *FASEB J.* **21,** 812–822
37. Hartshorne, D. A. (1987) in *Physiology of the Gastrointestinal Tract*, Second Ed., pp. 423–482, Raven Press, New York
38. Seto, M., Sasaki, Y., and Sasaki, Y. (1990) *Pflugers Arch.* **415,** 484–489
39. Patel, C. A., and Rattan, S. (2006) *Am. J. Physiol. Gastrointest. Liver Physiol.* **291,** G830–G837
40. Himpens, B., Matthijs, G., Somlyo, A. V., Butler, T. M., and Somlyo, A. P. (1988) *J. Gen. Physiol.* **92,** 713–729
41. Rattan, S., and Patel, C. A. (2008) *Am. J. Physiol. Gastrointest. Liver Physiol.* **294,** G687–G693
42. Yuen, S. L., Ogut, O., and Brozovich, F. V. (2009) *Am. J. Physiol. Heart Circ. Physiol.* **297,** H191–H199
43. Hirota, S., Helli, P., and Janssen, L. J. (2007) *Eur. Respir. J.* **30,** 114–133
44. Schelegle, E. S. (2003) *Anat. Rec. A Discov. Mol. Cell. Evol. Biol.* **270,** 11–16
45. Fanta, C. H. (2009) *N. Engl. J. Med.* **360,** 1002–1014
46. Hershenson, M. B., Brown, M., Camoretti-Mercado, B., and Solway, J. (2008) *Annu. Rev. Pathol.* **3,** 523–555
47. Diamant, Z., Boot, J. D., and Virchow, J. C. (2007) *Respir. Med.* **101,** 378–388